Article:
Liu, Q. and Ball, E. (2020) A tractable stochastic geometry model of coverage and an approach to energy efficiency estimation in LPWAN networks. International Journal of Sensor Networks, 33 (4). pp. 211-223. ISSN: 1748-1279

https://doi.org/10.1504/ijsnet.2020.109188

A tractable stochastic geometry model of coverage and an approach to energy efficiency estimation in LPWAN networks

Qiaoshou Liu

School of Communication and Information Engineering,
Chongqing University of Posts and Telecommunications,
Chongqing, China
E-mail: liuqs@cqupt.edu.cn

Edward A. Ball

Department of Electronic and Electrical Engineering,
The University of Sheffield,
Sheffield, UK
E-mail: e.a.ball@sheffield.ac.uk

Abstract: The low-power wide area network (LPWAN) is designed for low-power, wide area, light load, high latency applications. In many use-case applications of traffic being usually less than 1k of bytes transmitted data per day, it is desirable for a user equipment (UE) to work for 10 years, powered by a primary battery. There is neither real test data nor mathematical models to validate a 10 years battery lifetime. Furthermore, the energy consumption is affected by many factors and is very different in diverse networks. In this paper, we consider two types of LPWAN: LoRa wide area network (LoRaWAN) and narrow-band Internet of Things (NBIoT) network. We first propose a framework to calculate the average number of retransmissions in LoRaWAN networks and NBIoT networks based on stochastic geometry. Combining the average number of retransmissions, we give an approximate method to calculate both networks' energy efficiency. Utilizing the energy efficiency we can estimate the battery lifetime in LoRaWAN networks and NBIoT networks. The numerical results show that the battery lifetime is mainly influenced by the number of active UEs and the spreading factor in LoRaWAN networks and sleeping mode in NBIoT networks, when the data size transmitted each day is fixed. In NBIoT networks, the UEs can work for much longer with power saving mode (PSM) than with extended idle-mode discontinuous reception cycle (eDRX), even exceeding LoRaWAN networks in some cases though the transmitting power is higher and protocol is more complex in NBIoT networks. Finally, in LoRaWAN networks, smaller spreading factors can achieve longer battery lifetime, and increasing the number of base stations also extends the battery lifetime, which is not the case for NBIoT networks.

Keywords: LPWAN; LoRaWAN; NBIoT; Stochastic Geometry; PSM; eDRX.

Reference to this paper should be made as follows: Qiaoshou Liu, and Edward A. Ball 'A tractable stochastic geometry model of coverage and an approach to energy efficiency estimation in LPWAN networks', *International Journal of Sensor Networks*, Vol. x, No. x, pp.xxx–xxx.

Biographical notes: Qiaoshou Liu received his B.S. and M.S. degrees in communication engineering from Chongqing University of Posts and Telecommunications in 2002 and 2006, respectively, Chongqing, China. He is working toward his Ph.D. degree in communication and information at the National Key Laboratory of Science and Technology on Communication, University of Electronic Science and Technology of China, Chengdu, China. Currently, he is an associate professor at the School of Information and Communication Engineering, Chongqing University of Posts and Telecommunications. His research interests include interference management, ultra-dense networks, heterogeneous networks, stochastic geometry and IoT.

Edward A. Ball graduated in 1996 with a 1st Class Master of Engineering Degree in Electronic Systems Engineering, from the University of York, York, United Kingdom. After graduating, he worked in industry for 15 years as Principal RF Engineer at Cambridge Consultants Ltd in Cambridge, UK. He then spent 5 years as Principal RF Engineer and Radio Systems Architect at Tunstall Healthcare Ltd in Whitley, UK. In November 2015 he joined the Department of Electronic and Electrical Engineering at the University of Sheffield, Sheffield, United Kingdom, where he now works as Reader in RF Engineering. His research interests cover all areas of radio technology and the application of radio technology to real-world industrial and commercial problems. Mr. Ball is a member of the IET and is a Chartered Engineer.

1 Introduction

1.1 Motivation

The Internet of Things (IoT) era is now. A growing number of devices which involve various fields, are being connected to the Internet. Many reports forecast that the number of IoT devices will explosively grow in the next few years. In Gantz J. and Reinsel D. (2012); Taylor, S. (2013); Al-Fuqaha, A. et al. (2015), the authors predict that the IoT smart objects are expected to reach 212 billion entities deployed globally by the end of 2020. By 2022, machine-to-machine traffic flows are expected to constitute up to 45% of the whole Internet traffic. Economic growth of IoT-based services is also considerable for businesses. The whole annual economic impact caused by the IoT is estimated to be in range of 2.7 trillion to 6.2 trillion by 2025.

With the fast growth, IoT networks extend in two directions in the view of communication range. One is local area network: these networks mainly apply to healthcare, smart home, industrial automation, etc. by exploiting some short distance communication protocol such as radio frequency identification (RFID), Bluetooth, ZigBee and so on. These protocols support devices frequently accessing networks with low speed over a short distance area. The communication range is mostly from several metres to tens of metres and low mobility is permitted; the other is wide area networks, i.e. LPWAN. LoRaWAN networks and NBIoT networks are two typical but different LPWAN networks which are designed by LoRa alliance and the 3rd Generation Partnership Project (3GPP), respectively. LoRaWAN devices work with LoRa spread spectrum modulation, in the industrial scientific medical (ISM) band, and organized by pure Aloha protocol. In contrast, as a part of *Release* 13, NBIoT has been specified as a new radio interface by 3GPP. It is tightly connected with Long Term Evolution (LTE) but kept as simple as possible in order to reduce device costs and to minimize battery consumption by3GPP (2016).

In some applications, such as meter reading, environmental monitoring, smart agriculture and so on, the devices are deployed far away from their tagged base stations (or access points, gateways). The communication range is mostly from several hundred metres to tens of kilometres. The maximum area traffic capacity is more than 50k devices per cell Sinha, R. S. et al. (2017); Mekki, K. et al. (2018). The devices are often stationary, and only a small amount of data is transferred per day, which is not delay sensitive. Furthermore, devices are often installed at places without a power supply and work completely on batteries. The cost of changing batteries may be very expensive because huge numbers of devices are randomly deployed in a wide area, even then devices may only be accessed by trained staff. So, battery lifetime is a very important factor which must be firstly considered at the network design phase.

Both the LoRa alliance and 3GPP pushed the objective that devices should work more than 10 years with a battery supply for most applications because the cost of frequently changing batteries is unacceptable. It is proposed that a device just sends several hundred bytes per day, so the device can sleep most of the time to reduce the energy consumption. But, many factors decide the battery lifetime beside the transmitting load per day, such as the capacity of battery, bit rate, delay sensitive, interference and so on. Moreover, there is neither numerical models nor real measured data to support this goal.

In recent years, stochastic geometry as a tractable tool has been widely used to model and analyse the cellular networks. Most of these literatures focused on downlink (DL) and rapidly extend different hot spot fields, such as further enhanced inter-cell interference coordination (FeICIC) Hu, H.N. et al. (2016), coordinated multi-point transmission (CoMP) Nigam, G. et al. (2014), mm-Wave communication Andrews, J. G. et al. (2017), multi-input multi-output (MIMO) cellular networks George, G. et al. (2017), device-to-device (D2D) communication Salehi, M. et al. (2017) and so on.

For IoT devices, the data traffic mainly occurs in uplink (UL), i.e. from devices to base stations (or access points, gateways etc.), which is different from conventional cellular user equipments that mostly receive data from base stations. In fact, the stochastic geometry is more suitable for modelling and analysis of the IoT networks than cellular networks because the deployment of IoT devices is more random than the deployment of base stations in cellular networks.

1.2 Related work

In Kroll, H. et al. (2017), the authors proposed a maximum-likelihood detection to reduce the energy consumption in NBIoT networks. A wireless energy harvesting method was proposed to enhance the battery lifetime for IoT devices in Kamalinejad, P. et al. (2015). The authors predict the battery lifetime based on the power of the devices. In Lauridsen M. et al. (2015), the battery lifetime of LTE-M and NB-IoT was analysed in a rural area. The methods were too simple to accurately estimate the battery lifetime.

In Elsawy, H. and Hossain, E. (2014); Novlan, T.D. et al. (2013); Haenggi, M. (2016), the authors modelled and analysed the coverage probability of uplink cellular networks based on the Poission point process (PPP). Most of results in PPP uplink cellular networks can be directly used for NB-IoT networks because of their compatibility with cellular networks, but are not suitable for LoRaWAN networks. In Gharbieh, M. et al. (2016), the authors proposed a traffic-aware spatio-temporal mathematical model for IoT devices supported by cellular uplink connectivity. For LoRaWAB networks, a “card tossing” model was proposed to analyse the interference in 2 dimensional (time-frequency) plane

based on PPP Li, Z.C. et al. (2017). A special Aloha network, the bipolar model, was studied in Baccelli, F. et al. (2009). The authors derived the coverage probability and throughput exploiting a PPP model. The results of Aloha bipolar networks can not be directly used in LoRaWAN networks because the frame of Aloha bipolar networks is totally different from the LoRaWAN networks.

1.3 Contributions

In this paper, we aim at investigating the coverage probability, analysing the energy efficiency and estimating the battery lifetime in LPWAN networks based on PPP. The main contributions of this paper are summarized in the following:

(a) We propose a novel analysis framework for UL in LoRaWAN networks. Based on this model, we derive the coverage probability of UL in LoRaWAN networks.

(b) We propose a simple, but more accurate, homogeneous Poisson point process to model the interferers in the UL of the NBIoT networks, then deriving the coverage probability of UL in NBIoT networks.

(c) We calculate the average number of retransmissions based on coverage probability, leading to our energy efficiency model. Our energy efficiency models represent the key characteristics of LoRaWAN networks and NBIoT networks.

(d) We estimate the battery lifetime utilizing our energy efficiency model. The numerical results show an example of the battery lifetime according to a LoRaWAN hardware module and a NBIoT hardware module.

The remainder of the paper is organized as follows: In Section II we propose our system model for LPWAN networks, then discuss this model for LoRaWAN networks and NBIoT networks, respectively. We derive the coverage probability and the average number of retransmissions in UL for LoRaWAN networks and NBIoT networks in Section III. The energy efficiency model is proposed in Section IV. Then, the energy efficiency model is tailored for LoRaWAN networks and NBIoT networks. Based on our energy efficiency model, we present the approach to estimate the battery lifetime. In Section V, we validate our numerical coverage probability results with Monte Carlo simulation results. Furthermore, we compare the energy efficiency and battery lifetime between LoRaWAN networks and NBIoT networks. The conclusions are given in Section VI.

2 System Model

In this paper, we only consider the class A devices in LoRaWAN networks. We uniformly denote the device in LoRaWAN networks and NBIoT networks as UE, denote the gateway (or access point) in LoRaWAN networks and eNB in NBIoT networks as base station (BS). We consider all UEs working with two modes: sleep mode and active mode. In sleep mode, UEs turn off most of their functional modules, especially those of the radio module to reduce the energy consumption. In active mode, UEs turn on all of their functions so that they can communicate with the networks. In NBIoT networks, a UE can select from two types of sleep modes and the active mode includes two states, all of which will be described later. In our use-case, we consider a single-tier uplink LPWAN network model in a given area of $\mathbb{R}^2$ for both LoRaWAN networks and NBIoT networks, where BSs and UEs are randomly deployed according to some homogeneous Poisson point process Φ_b and Φ_u with density of λ_s and λ_u, respectively, i.e. $\Phi_s \sim \text{P.P.P.}(\lambda_s)$ and $\Phi_u \sim \text{P.P.P.}(\lambda_u)$. Furthermore, all UEs are located at fixed positions at deployment and choose their closest BSs (the nearest BSs in Euclid distance) to communicate, which means handover is not need. In UL, all UEs access their tagged BSs with fixed transmit power P_{tx}. The number of UEs is much more than the number of BSs, the LPWAN is a fully loaded network, i.e. at least one UE in each cell is served in a fixed time-frequency resource. For notational convenience, we denote BSs and UEs by their locations. Without loss of generality, we consider a typical BS located at the origin and denoted by s_o. Let $V(s_o) = \left\{x \in \mathbb{R}^2 : \|s_o - x\| \leq \|z - x\|, \forall z \in \Phi_s \backslash \{s_o\}\right\}$ denote the Voronoi Cell (VC) of s_o. For the typical BS s_o, the signal to interference plus noise (SINR) from a UE located at x_j is defined as

$$\text{SINR}_j = \frac{P_{tx} h_{x_j} \|x_j\|^{-\alpha}}{\sum\limits_{x_i \in \Phi_{\text{I}}} P_{tx} h_{x_i} \|x_i\|^{-\alpha} + \sigma^2}, \quad x_j \in V(s_o). \quad (1)$$

Where $\|\cdot\|$ denotes the Euclid distance in $\mathbb{R}^2$, $\alpha > 2$ is the path loss exponent, h_x is the small scale fading loss. In this paper, we assume that BSs and UEs only experiences Rayleigh fading with unit mean, and all h_x are exponential independent and identically distributed (i.i.d.), i.e. $h_x \sim \exp(1)$. Φ_{I} is the set of all interfering UEs in the network. We treat x_j as the typical UE for any a given j. Φ_{I} and the typical UE will be separately discussed for LoRaWAN networks and NBIoT networks later.

For LPWAN networks, UEs must turn off most of their functional modules, especially the RF module, and enter into sleep mode to reduce energy consumption when there is no data to be sent. Simply, let p_a denote the composite UE activity probability, i.e. there are $p_a \cdot N_u$ UEs sending messages to their tagged BSs at the same time, where N_u is the total number of UEs in the network. According to the Thinning theorem François B. et al. (2009), the set of active users Φ_a is still a PPP with density of $p_a \lambda_u$, i.e. $\Phi_a \sim \text{P.P.P.}(p_a \lambda_u)$.

2.1 The set of interferers and the typical UE of LoRaWAN networks

In LoRaWAN networks, UEs access their tagged BSs obeying pure Aloha protocol with duty cycle $< 1\%$, LoRa Alliance (2016). Any of the active UEs send messages to their tagged BSs on a randomly chosen channel from N_c channels and N_f spreading factors (SFs), N_c and N_f are the number of total RF channels and the number of total SFs, respectively, which are used by LoRaWAN networks. As mentioned above, we treat x_j, which belongs to the $V(s_o)$, as the typical UE for a given j in Eq. (1). All other active UEs using the same channel with the same SF act as interferers. The probability of the active UEs simultaneously transmitting data in the same channel with the same SF is $1/(N_c \cdot N_f)$. Let Φ_{sc} denote the set of all active UEs that simultaneously transmit data in a same channel with a same SF. Based on the thinning theory, Φ_{sc} is still a PPP with density of λ_a, which can be expressed as

$$\lambda_a = \frac{p_a \cdot N_u}{N_c \cdot N_f}. \tag{2}$$

For the typical user x_j, the interfering set is $\Phi_{\mathrm{I}} = \Phi_{sc} \backslash \{x_j\}$. Considering the UL of LoRaWAN networks, on the one hand, there is both intra-cell interference and inter-cell interference. On the other hand, some interfering UEs may be much closer to the typical BS s_o than the desired UE x_j. According to the reduced Palm distribution, Martin H. (2012), adding x_j into Φ_{sc} does not change the original distribution of the Φ_{sc}. So, we can redefine the $\Phi_{\mathrm{I}} = \Phi_{sc}$ but with density of $\lambda_i = 2 \cdot \lambda_a$ because the collision time is twice the sending cycle in a pure Aloha system (LoRaWAN network), i.e. the λ_i cen be expressed as

$$\lambda_i = 2 \cdot \lambda_a = \frac{2 \cdot p_a \cdot N_u}{N_c \cdot N_f}. \tag{3}$$

2.2 The set of interferers and the typical UE of NBIoT networks

In NBIoT networks, at the initial stage, a UE camps on a BS (the closest BS and with no handover) by searching a cell on an appropriate frequency, reading the associated system information block (SIB), then starting a random access channel (RACH) procedure to register with the network. After camping on a BS, the UE leaves sleep mode and enters into active mode if it has some data to send. Since handover is not supported when the UE is in active mode and connected with a BS, the state model of the radio resource control (RRC) becomes simple, with only two states: *RRC_CONNECTED* and *RRC_IDLE* 3GPP (2016). In *RRC_CONNECTED* state, UEs start connection request and communication with BSs. In *RRC_IDLE* state, UEs receive paging information from BSs.

NBIoT networks are different from LoRaWAN networks (where UEs send message directly to the networks); in NBIoT networks, UEs must transmit data under the schedule of the network. There is only one UE permitted to send its message to its tagged BS using a particular time-frequency Resource Unit (RU is a smaller resource for NBIoT devices than a Resource Block) in each cell. This means there is no intra-cell interference but there may be inter-cell interference, with only one interferer in each other cell. Let Φ_{cc} denote the set of all UEs which simultaneously transmit data in the same RU in each VC (1 UE per VC). Hence Φ_{cc} is still a PPP with the same density of BS, i.e. $\Phi_{cc} \sim \mathrm{P.P.P.}(\lambda_s)$. For the typical user x_j, the interfering set $\Phi_{\mathrm{I}} = \Phi_{\mathrm{cc}} \backslash \{x_j\}$. In this case, it is worth mentioning that when a typical UE was chosen, the interferers surely belong to other VCs. This means that the reduced Palm distribution can not be applied to this situation as was used in LoRaWAN networks.

Many works have been done to model and analyse the distribution of active UEs in UL of cellular networks. In ElSawy, H. and Hossain, E. (2014), the authors modelled the interfering UEs as a homogeneous PPP. However the typical user is not an interferer, in this case, the interfering UEs process is not a homogeneous PPP but a soft-core process whose density depends on the distance from the origin Lee H. Y. et al. (2017); Singh, S. et al. (2015). In Haenggi, M. (2017), the author modelled this soft-core process with an approximation to a density function, which is given as

$$\lambda_{\mathrm{I}}(x) = \lambda_s(1 - \exp(\lambda_s \pi \|x\|^2)). \tag{4}$$

Furthermore, in Wang, Y.J. et al. (2017), the authors proposed a more accurate approximation of a density function based on Haenggi, M. (2017) to model the interfering UEs as a non-homogeneous PPP, and the density function was expressed as

$$\lambda_{\mathrm{I}}(x) = \lambda_s(1 - \exp((-12/5)\lambda_s \pi \|x\|^2)). \tag{5}$$

Modelling the interfering UEs as a non-homogeneous PPP is an accurate method, but it will lead to much more computation complexity. To compensate the error in the model of homogeneous PPP with the same density of BS. In Bai, T., and Heath, R.W. (2016), the authors approximated interfering UEs as a homogeneous PPP excluding the ball centred at the typical BS with the radius $R_e = 1/\sqrt{\lambda_s \pi}$. This is a simple but more precise model than the standard homogeneous PPP. Due to the set of BSs being a homogeneous PPP and UEs being randomly deployed in the network, the average distance from UEs to their closest BSs is $1/\left(2\sqrt{\lambda_s}\right)$. So we can assume the average distance between interfering UEs and the typical BS is farther than $1/\left(2\sqrt{\lambda_s}\right)$. In this paper, we model the interfering UEs by a homogeneous PPP excluding the ball centred at the typical BS with the radius $1/\left(2\sqrt{\lambda_s}\right)$, i.e. $\Phi_{\mathrm{I}} = \Phi_s | \left(\|x_i\| \geq 1/\left(2\sqrt{\lambda_s}\right), \forall x_i \in \Phi_{\mathrm{I}}\right)$.

We normalized $\lambda_s = 1$ BSs/km^2 as $\lambda = 1$, then verify these approximation methods by inspecting Ripley's K function Martin H. (2012) in Fig. 1, clearly showing

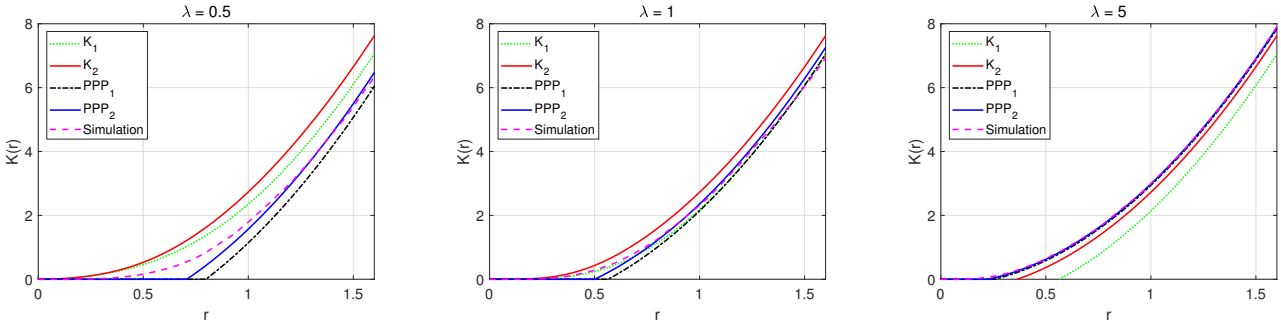

(a) $\lambda = 0.5$ (b) $\lambda = 1$ (c) $\lambda = 5$

Figure 1: Ripley's K function. $K_1(r) = \pi r^2 + 5/12e^{-12/5\lambda\pi r^2} - 5/12$ and $K_2(r) = \pi r^2 + e^{-\lambda\pi r^2} - 1$ corresponding to Eq. (4) and (5), respectively. PPP_1 and PPP_2 are K functions of homogeneous PPP excluding the ball with radius $1/\left(2\sqrt{\lambda}\right)$ and $1/\left(\sqrt{\lambda\pi}\right)$. All K functions are compared with the simulation of interfering UEs.

that the precision of four approximate approaches relates to the density of BSs. As shown in Fig. 1, the two approaches of non-homogeneous PPP overestimate the number of interferers when λ is small, and underestimate the number of interferers when λ is large. Furthermore, the two approaches of homogeneous PPP with an excluding ball centred at the analysed BS is more close to the simulation result when λ is large. Our approximate model is the best trade-off of the four approaches.

3 Coverage Probability

For notational convenience, we omitted the subscript in Eq. (1), hence let random variable (r.v.) R denote the distance between the typical UE x_j and the typical BS b_o. The distance between interfering UE x_i and the typical BS b_o is denoted by r.v. R_x, i.e. $R = \|x_j\|$ and $R_x = \|x_i\|$, respectively. Conventionally, cellular networks have been considered as thermal noise limited networks, Andrews, J.G. et al. (2011). The transmit power of LPWAN UEs is less than that of connventional cellular UEs, but the transmit power spectral density of LPWAN UEs is much larger than that of conventional cellular UEs because the LPWAN UEs use very narrow bandwidth in both DL and UL. Thus, neglecting the noise, we rewrite Eq. (1) as follows:

$$\text{SIR} = \frac{hR^{-\alpha}}{\sum\limits_{x\in\Phi_{\text{I}}} h_x R_x^{-\alpha}}. \tag{6}$$

We define the coverage probability as the probability $\mathbb{P}(\text{SIR} > T)$, this means that a randomly chosen BS can demodulate the received signal if and only if the SIR exceeds a predefined threshold T.

Theorem 1: *Assume in LPWAN networks the BSs are deployed according to a homogeneous PPP with density of λ_s and UEs are uniformly located in the network with density of λ_u. The probability of active UEs is p_a, All UEs transmit data to their closest BSs with a fixed power P_{tx}. When neglecting thermal noise, the coverage probability of the LoRaWAN networks is*

$$P_c(T) = \frac{\alpha N_c N_f \lambda_s}{p_a \lambda_u T^{2/\alpha} \cdot 4\pi \cdot \csc\left(\frac{2\pi}{\alpha}\right) + \alpha N_c N_f \lambda_s}. \tag{7}$$

The coverage probability of NBIoT networks is

$$P_d(T) = \int_0^\infty e^{-\left(1+T^{2/\alpha}\cdot F(x)\right)x} dx. \tag{8}$$

Where

$$F(x) = \int_{\frac{\pi}{4xT^{2/\alpha}}}^\infty \frac{1}{1+u^{\alpha/2}} du. \tag{9}$$

P: for proof please see Appendix A. □

For LoRaWAN networks, the coverage probability of the UL is different to that in DL where coverage probability is influenced by neither the density of BSs nor UEs. In UL, Eq. (7) shows the coverage probability is affected by both the density of BSs and density of UEs and probability of UE activity. In UL, increasing the number of UEs (or more UE activity) will lead to more interference but the average distance from UEs to their closest BSs remains unchanged when the density of BSs is fixed. Thus, the coverage probability is a decreasing function of both the density of UEs and the probability of active UEs. In contrast, increasing the density of BSs will reduce the average distance from UEs to their closet BSs but the interference remains, since the density of UEs and the probability of active UEs is fixed. The coverage probability is an increasing function of the density of BSs.

For NBIoT networks, the coverage probability is influenced by neither the density of BSs nor UEs as show in Eq. (8). This is because the UEs are scheduled by the network, and there is no intra-cell interference and only one random interferer from each other cell.

4 Energy efficiency

In LoRaWAN networks and NBIoT networks, all UEs transmit data with frequency division (FD) half-duplex mode. The energy consumption of a UE mainly includes three parts: the energy consumption of the processor, the energy consumption of RF circuit in transmission, and the energy consumption of RF circuit in reception. In LPWAN networks, most communications occur in UL. Hence, in this paper, we focus on the energy efficiency of transmission in UL.

In section 2, we assume that all UEs transmit data to their tagged BSs with the fixed power P_{tx}. In the real LPWAN networks, especially in NBIoT networks, the transmitting power depends on a combination of cell-specific parameters, the selected RU and UE measured parameters, 3GPP (2016). It is complicated to model and calculate the energy consumption based on dynamic power control. Furthermore, the radio frequency integrated circuit (RFIC) used in LPWAN networks can only provide a few transmitting power levels. So, we maximize the energy consumption by considering the worst case where all UEs transmit data with the fixed maximum power P_{tx} for all transmissions. The resulting energy efficiency from this paper can hence be considered an approximation of the energy efficiency, which provides a guide for designing the real networks.

Before studying energy efficiency, we must predict the average number of retransmissions that a typical UE will use in successfully sending a message to its tagged BS. In UL, if the set of active UEs which simultaneously transmit data is the same each time, it will lead some UEs unable to send messages to their tagged BSs if the required SIR threshold for demodulation is more than 0dB. This is because there are some interfering UEs much closer to these UEs' tagged BSs. In this case, the number of retransmissions of these UEs is infinite. Furthermore, all the UEs send messages driven by events, so the transmission process can be considered a stationary process where every UE will be randomly chosen to send a message with probability of λ_a. This means different sets of UEs transmit data simultaneously at different times, which avoids the case that some UEs can never send messages to their tagged BSs.

Let r.v. N_{scf} denote the number of retransmissions, p denotes the successful probability of each transmission and $q = 1 - p$ denotes the failed probability of each transmission, hence the average number of retransmissions is given as

$$N_{av} = \mathbb{E}\left[N_{scf}\right] = \sum_{i=1}^{\infty} i \cdot q^{i-1} \cdot p = p^{-1}. \tag{10}$$

In section 3, the coverage probability is the spatial average successful probability of the UEs accessing their tagged BSs. Let $p = P_c$ for LoRaWAN networks; and let $p = P_d$ for NBIoT networks. We can define the energy efficiency as the number of bits which successfully transmit in UL with unit energy consumption expressed as

$$\begin{aligned} EE &= \frac{N_u \cdot M \cdot D_{tx}}{N_u \cdot N_{av} \cdot M \cdot E_{tx}\,(1+\beta) + N_u \cdot E_{other}} \\ &= \frac{1}{N_{av}} \cdot \frac{R_{tx}}{P_{tx} \cdot (1+\beta) + \frac{R_{tx} \cdot E_{other}}{N_{av} \cdot M \cdot D_{tx}}} \\ &= p \cdot \frac{R_{tx}}{P_{tx} \cdot (1+\beta) + \frac{p \cdot R_{tx}}{M \cdot D_{tx}} \cdot E_{other}} \\ &= p \cdot N_{pbj}. \end{aligned} \tag{11}$$

Where, M denotes the average number of transmissions in UL each day, and D_{tx} is the length (in bits) of data. We assume that each UE transmits the same size data each time in UL. E_{tx} denotes the energy consumption for transmitting the data D_{tx} once. β is the energy coefficient which is used to represent the energy consumption of signaling transmission, acknowledgement (ACK) reception and is influenced by the length of transmitting data. E_{other} denotes some other energy consumption which will be discussed later. R_{tx} is the physical bit rate (in bits/s) in UL. N_{bpj} is the number of bits that can be transmitted with a unit energy consumption without considering the retransmission. To get the energy efficiency based on Eq. (11), we only need to derive the N_{bpj}. This is very different for LoRaWAN networks and NBIoT networks because the difference of their media access control (MAC) protocol and RFIC.

4.1 LoRaWAN networks

In this paper, we only consider basic UEs in LoRaWAN networks, i.e. end-devices of Class A, which allow for bidirectional communications whereby each end-device's uplink transmission is followed by two short receive windows as shown in Fig. 2. In LoRaWAN networks, all end-devices must implement Class A features.

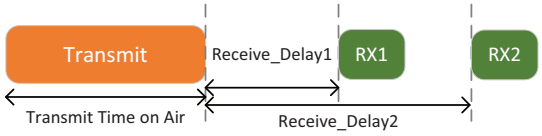

Figure 2: Class A device receive slot timing in LoRaWAN networks.

In LoRaWAN networks, UEs directly send messages to their tagged BSs. If the transmission fails, they will retransmit the messages again after a period defined by the duty cycle, until reaching the maximum number of retransmissions, which is not in the scope of this paper. For power saving, LoRaWAN UEs asynchronously communicate with the BSs. There is no other excess energy consumption, so we can let $E_{other} = 0$. Furthermore, since LoRaWAN is a simple communication protocol, little energy is consumed for signaling transmission and ACK reception, so we can

set β as a positive number close or equal to zero, which minimizes influence on the results. So, N_{bpj} for LoRaWAN can be simplified to

$$N_{bpj} = \frac{R_{tx}}{P_{tx} \cdot (1+\beta)}. \quad (12)$$

Where R_{tx} for different spreading factor can be obtained from LoRa Alliance (2016). In the datasheet of SX127x Semtech Co. (2015), an accurate method is provided for obtaining T_{tx}. SX127x is widely used for LoRaWAN networks and is produced by Semtech Ltd. x equals either 6,7,8,9-relevant to different countries with different frequency bands. These RFICs support both LoRa, FSK, and OOK modulation. In this paper, we focus on the investigation of energy consumption when the IC transmits data with LoRa spread spectrum modulation. In LoRaWAN networks, the UL messages always start with a programmed preamble. For LoRa spread spectrum modulation, the duration of a symbol is

$$T_s = \frac{2^{SF}}{BW}. \quad (13)$$

Where SF is the spreading factor and BW is the programmed Tx bandwidth. The LoRaWAN packet duration is the sum of the duration of the preamble and the data packet. The preamble length is calculated as follows:

$$T_{preamble} = (n_{preamble} + 4.25) \cdot T_s. \quad (14)$$

Where $n_{preamble}$ is the programmed preamble length. The following formula gives the number of payload symbols.

$$n_{payload} = 8 + \max\left(ceil\left[\frac{(8PL - 4SF + 28 + 16CRC - 20IH)}{4(SF - 2DE)}\right](CR+4), 0\right). \quad (15)$$

PL is the number of payload bytes (1 to 255), SF is the spreading factor (6 to 12), IH is the enable flag of header, DE is the enable flag of $LowDataRateOptimize$, CR is the coding rate (1 corresponding 4/5, 4 to 4/8), CRC is the enable flag of cycle redundancy check. For more details refer to Semtech Co. (2015).

The payload duration is then the symbol period multiplied by the number of payload symbols

$$T_{payload} = n_{payload} \cdot T_s. \quad (16)$$

The time on air is simply the sum of the preamble and payload duration (in second).

$$T_{packet} = T_{preamble} + T_{payload}. \quad (17)$$

Based on the Eq. (17) and (11), we can obtain the N_{bpj} in LoRaWAN networks as

$$N_{bpj} = \frac{8PL}{U \cdot I_{tx} \cdot T_{packet} \cdot (1+\beta)}. \quad (18)$$

Where U is the power supply voltage (in Volts) of the IC, and I_{tx} is the transmitting mode current (in Amperes) of the IC. Comparing with Eq. (12), (18) provides a more precise realization of energy efficiency measurement. Furthermore, using $U \cdot I_{tx}$ instead of the RF transmitting power incorporates the effects of RF amplifier and processing energy consumption in the model.

4.2 NBIoT networks

NBIoT Networks utilize two sleep methods to conserve battery power: power saving mode (PSM) and extended idle-mode discontinuous reception cycle (eDRX) as shown in Fig. 3 and Fig. 4, respectively. PSM provides more power saving but higher latency, eDRX provides less power saving but low latency. PSM was proposed in 3GPP Release 12 and is specified in 3GPP TS24.301 3GPP (2017) and TS23.682 3GPP (2017). In Fig. 3, the maximum tracking area updating period (T3412) is decided by the network. The maximum time a device may be reachable is 186 minutes (equivalent to the maximum value of the active timer T3324). For more details about T3412 and T3324 refer to 3GPP (2017, TS23.682, TS24.008, TS24.301).

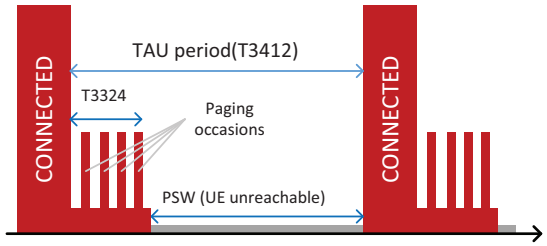

Figure 3: The power profile of a NBIoT UE in PSM mode.

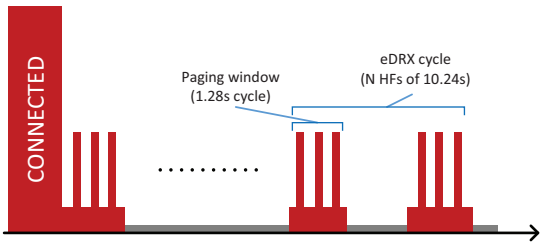

Figure 4: The power profile of a NBIoT UE in eRDX mode.

In PSM, UEs turn off their RF modules and enter into dormant state to reduce the energy consumption. This mode is similar to power-off, but UEs remain registered with the network and there is no need to re-attach or re-establish PDN connections 3GPP (2017). When a UE wakes up from PSM, it uses its stored access statum (AS) context (which was obtained from the network at the last paging), to transmit data. Afterwards, the UE returns to the RRC_IDLE state, from where it may either use the RACH procedure if it has mobile originated data to send, or waits until it gets paged 3GPP (2016). The UE will leave RRC_IDLE state and enter into PSM if the

UE does not operate or not receive any data from the BS in a period which is defined by the network.

In the above case, the E_{other} in Eq. (11) denotes the energy consumption of paging which occurs at the RRC_IDLE state and its duration is defined by T3324. As shown in Fig. 3, paging always occurs after $RRC\_CONNECTED$. The N_{bpj} for NBIoT UEs which exploit PSM to reduce energy consumption is given as

$$\begin{aligned} N_{pbj} &= \frac{R_{tx}}{P_{tx}\cdot(1+\beta)+\frac{p\cdot R_{tx}}{M\cdot D_{tx}}(M\cdot P_{rx}\cdot T_p)} \\ &= \frac{R_{tx}}{U\cdot I_{tx}\cdot(1+\beta)+\frac{p\cdot R_{tx}}{D_{tx}}\cdot(U\cdot I_{rx}\cdot T_p)}. \end{aligned} \tag{19}$$

Where $P_{rx} = U \cdot I_{rx}$ denotes the UEs consumed power when in RF receive mode, I_{rx} is the average DC current when the UE is in receive mode. T_p is the duration of the paging window.

LTE networks exploit discontinuous reception (DRX) cycle to save paging power. The eDRX is an extension of an existing LTE feature which can be used by NBIoT UEs to reduce power consumption. A normal LTE paging cycle is 1.28s 3GPP (2017), the not-yet-implemented LTE DRX improvement to LTE will allow UEs to sleep for 10.24s between paging cycle. As shown in Fig 4, the eDRX innovation allows the UEs to tell the network how many "hyper frames" (HFs) of 10.24s it would like to sleep before resuming paging 3GPP (2017). The maximum number of HFs a UE can sleep is defined by the mobile network operator. In this case, the N_{bpj} for NBIoT UEs which exploit eDRX to reduce energy consumption is given as

$$\begin{aligned} N_{pbj} &= \frac{R_{tx}}{P_{tx}\cdot(1+\beta)+\frac{p\cdot R_{tx}}{M\cdot D_{tx}}(M\cdot P_{rx}\cdot T_p+N_p\cdot P_{rx}\cdot T_p)} \\ &= \frac{R_{tx}}{U\cdot I_{tx}\cdot(1+\beta)+\frac{p\cdot R_{tx}}{D_{tx}}\cdot((1+N_p/M)\cdot U\cdot I_{rx}\cdot T_p)}. \end{aligned} \tag{20}$$

where N_p is the number of paging events each day, which can be expressed as

$$N_p = floor\left(\frac{24\times 60\times 60}{N\times 10.24}\right). \tag{21}$$

where N is the number of hyper frames, i.e. the interval between two adjoined paging events.

At the $RRC\_CONNECTED$ state, a UE must request connection before sending messages. In some environments, it may enter into RRC_IDLE to start RACH procedure, for more details refer to 3GPP (2016). This means there is an energy cost in exchanging signaling between UEs and their tagged BSs. Hence, we can not get a precise model of N_{pjb} in a similar way to the LoRaWAN networks and the value of β in Eq. (19) and (20) must be set larger than that in Eq. (12) or (18) to compensate the energy consumption of signaling exchange and RACH procedure.

With the energy efficiency, we can estimate the battery lifetime by

$$B_{life} = \frac{3600\cdot U_{dr}\cdot C_{bat}\cdot\eta}{365\cdot(E_{sl}+M\cdot E_{dc}+M\cdot D_{tx}/EE)}, \tag{22}$$

Table 1 Parameters for coverage probability

Parameter	Description	Value
λ_s	Density of BSs	$1\,\mathrm{BSs/km^2}$
λ_u	Density of UEs	$10\mathrm{k\,UEs/km^2}$
α	Path loss Exponent	4
N_c	Number of sub-channels	8
N_f	Number of spreading factors	6
P_{tx}	Transmitting Power of UEs	20 dBm
S	Area of network for simulation	5km × 5km

where U_{dr} is the valid voltage range of battery, i.e. the voltage drop from the highest voltage to the lowest voltage ensuring the device working, C_{bat} is the capacity of battery (in Amp-hours), η is the transfer efficiency of the power supply unit (PSU); E_{sl} is the energy consumption of a device in sleep mode per day, $M \cdot E_{dc}$ is the energy consumption of a device collecting data per day (before sending), $M \cdot D_{tx}/E_{eff}$ is the energy consumption of a device sending data per day. The E_{sl} is defined as

$$E_{sl} = 24\cdot 3600\cdot U\cdot I_{sl}, \tag{23}$$

and the E_{dc} is defined as

$$E_{dc} = U\cdot I_{act}\cdot T_{act}, \tag{24}$$

where U is the device typical supply voltage in units of Volt, I_{sl} is the average current in units of Ampere that the device uses in the sleep mode, I_{act} is the average current in units of Ampere that the device uses in the active mode, T_{act} is the data collecting time in unites of seconds. Then from the Eq. (22), we can obtain an approximation of the battery lifetime (in years) ignoring the self-discharge of battery (typically about 1% per year for primary cellsBurdett A. (2015)).

5 Numerical Results

In this section, we validate our numerical results of the coverage probability with Monte Carlo simulations. In the simulation, the BSs and UEs are randomly deployed in a 5km × 5km area of $\mathbb{R}^2$. The transmitting power of the UEs does not influence the coverage probabilities because we neglect the effect of thermal noise. The main parameters are given in table 1.

Fig. 5 shows how the coverage probabilities vary with the demodulator SIR threshold. Solid lines denote the numerical results and dotted lines denote the Monte Carlo simulation results. As shown in Fig. 5, the coverage probabilities of LoRaWAN networks will descend when the number of active UEs increases. For NBIoT networks, the coverage probabilities of NBIoT networks is not influenced by the number of active UEs due to the scheduler. When the density of BSs is larger, the numerical result is closer to the Monte Carlo simulation results. This is consistence with Fig 1. Furthermore, the density of BSs slightly influences

Table 2 Parameters for modulations

Modulation	Demodulator SIR	Data length
$QPSK$	10 dB	125 Bytes
$SF7$	−7.5 dB	125 Bytes
$SF8$	−10 dB	125 Bytes
$SF10$	−15 dB	50 Bytes
$SF12$	−20 dB	50 Bytes

the coverage probability, though it is always neglected in both the homogeneous PPP model and the non-homogeneous PPP.

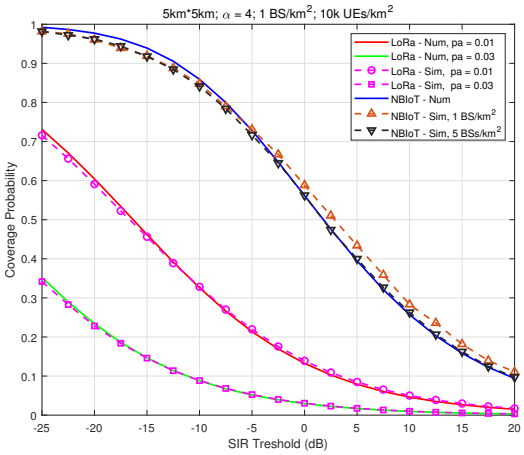

Figure 5: The coverage probability of LoRaWAN will reduce with increasing numbers of active UEs. The coverage probability of NBIoT networks is not influenced by the number of active UEs. Average 10k UEs/cell.

As discussed in section 4, we need the average number of retransmissions (which is the inverse of the coverage probability), to calculate the energy efficiency and hence estimate the battery lifetime. Obviously, it is unfair to calculate the coverage probability using the same demodulator SIR threshold for different modulations. Furthermore, the maximum size of payload varies with system. Based on 3GPP (2016); LoRa Alliance (2016); Semtech Co. (2015), we focus on SF7, SF8, SF10, SF12 spread spectrum modulations in LoRaWAN networks and only consider data transmission with QPSK modulation in NBIoT networks (in UL of NBIoT networks, BPSK and QPSK are supported: control data is transmitted with BPSK modulation and user data mostly transmitted with QPSK modulation). The parameters for demodulator SIR thresholds and payload size are set up as shown in the table 2.

Fig. 6 illustrates the coverage probabilities in LoRaWAN networks due to changing the density of BSs, when the density of UEs and the probability of active UEs is fixed. Solid lines denote the numerical results and dotted lines with squares denote the Monte Carlo simulation results. The figure shows that when the spreading factor is larger, the probability is higher, but increases only slowly as a function of BSs density.

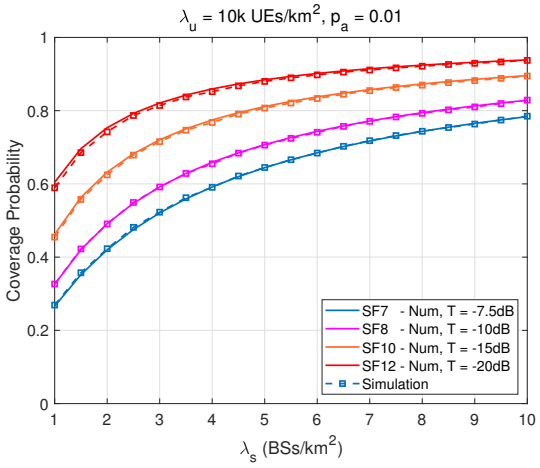

Figure 6: The coverage probability of LoRaWAN networks will increase with the increasing of BSs density for a fixed number of active UEs. Average 10k UEs/cell.

Table 3 Parameters for LoRa networks

Parameter	Description	value
U	Typical power supply	3.3 V
I_{tx}	Average current @ $P_s = 20$ dBm	120 mA
I_{sl}	Average current @ active mode	5.8 mA
I_{act}	Average current @ sleep mode	1.5 uA
BW	Bandwidth	125 kHz
IH	Header enable	1
DE	Low data rate optimize	1
CR	Code rate	4/5
CRC	Cyclic redundancy check enable	1
$n_{preamble}$	Number of preamble	8

Table 4 Parameters for NBIoT networks

Parameter	Description	value
U	Typical power supply	3.6 V
I_{tx}	Average current @ $P_s = 23$ dBm	220 mA
I_{rx}	Average current @ receive mode	46 mA
I_{sl}	Average current @ active mode	6 mA
I_{act}	Average current @ sleep mode	3 uA
R_{tx}	maximum bit rate in UL	62.5 kbps
M	Transmissions per day	2
N	Number of HFs	500

To observing the energy efficiency, we set the parameters in Eq. (18) based on Semtech Co. (2015) as show in table 3, and set the parameters in Eq. (19) and Eq. (20) based on Ublox Ltd. (2017) as show in table 4. We assume that both UE types work with the maximum RF output power, and the NBIoT UEs transmit with the maximum bit rate in UL (due to lack of interference in the licensed spectrum and only one interferer in each other cell).

The duration of the paging window (T_p in (19)) is 5.12 seconds (4 paging occasions with 1.28s cycle) if UEs utilize PSM to save power. The duration of the paging window (T_p in (20)) is 3.84 seconds (3 paging

occasions with 1.28s cycle) if NBIoT UEs utilize eDRX to save power. The number of HFs is 500, which overall means that the interval of paging is 500×10.24 seconds, approximates 1.42 hours. The value of data collecting time (T_{dc}) varies depending on application. We set the $T_{dc} = 1$ *second* as a reference value because it is sufficient for most data collecting. The energy consumption for data collecting is much less than the energy consumption for data sending in wireless systems.

Fig. 7 shows how the energy efficiency varies with the payload size. The energy efficiency of LoRaWAN networks is almost constant when the payload size is larger than 30 bytes. But the energy efficiency of NBIoT networks varies rapidly with the payload size, especially for PSM. This is because UEs consume a lot of energy transmitting signaling, paging or RACH scheduling. Increasing payload size increases the ratio of energy consumption. Meanwhile, transmitting smaller data block will cost more energy in NBIoT networks than in LoRaWAN networks.

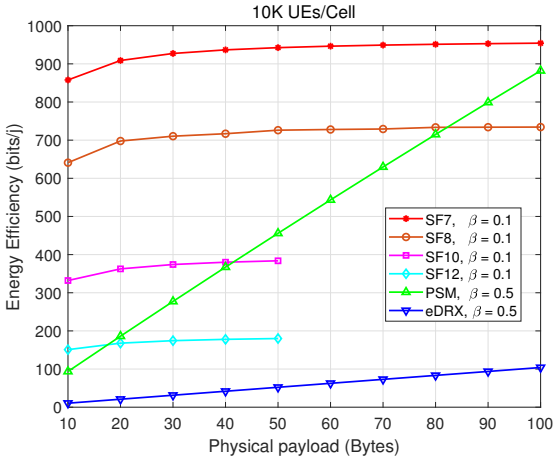

Figure 7: How the energy efficiencies vary with UEs' payload size for various SF in LoRaWAN and NB-IoT networks.

Fig. 8 shows how the energy efficiency varies with the energy coefficient β. As discussed in Section 4.1, LoRaWAN is a simple communication protocol, and the end-devices of Class A rarely exchange signaling with the network after joining with a BSs. In this case, the β must be set close to zero. For example, the energy efficiencies are reduced by about 10.7% when β varies from 0 to 0.1.

In NBIoT networks, the impact of β on energy efficiency is much smaller, the energy efficiencies of PSM is reduced by about 5.2% and the energy efficiency of eDRX is reduced by about 0.61% when β is from 0 to 1 in NBIoT networks. This is because NBIoT UEs spend significant energy paging in addition to transmitting data and signaling. The energy efficiency of PSM is much higher than that of eDRX, this is because UEs spend more energy paging to reduce the latency in eDRX.

Fig. 9 illustrates the energy efficiency of different SFs in LoRaWAN networks and different sleep modes

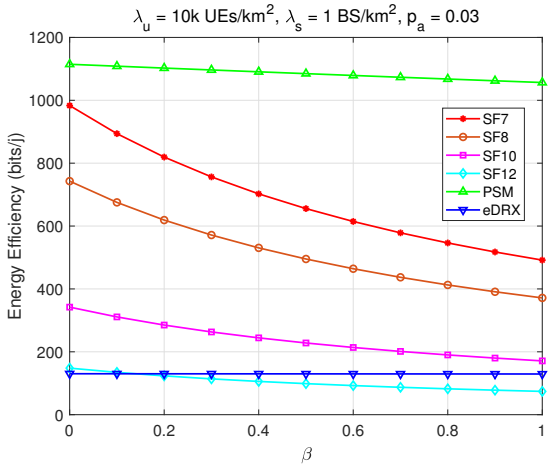

Figure 8: The energy efficiencies vary with the energy coefficient β.

in NBIoT networks. For LoRaWAN networks, we set $\beta = 0.1$: the blue bars denote that the probability of active UEs p_a is 0.01 and yellow bars denote $p_a = 0.03$. As shown in the Fig. 9, when the spreading factor is smaller, the energy efficiency is larger. This is because smaller SF means higher bit rate, with reduced time for data transmitting and attendant reduced energy consumption. This observation is consistent with the Eq. (11).

For NBIoT networks, the probability of active UEs does not influence the average number of retransmission. UEs must request connection before sending messages, so the energy coefficient β must be set much larger than that in LoRaWAN networks, though it only slightly influences the energy efficiency as shown in Fig. 8. The blue bars in Fig 9 denote $\beta = 0.5$ and the yellow bars denote $\beta = 1$. As shown in Fig. 9, $\beta = 1$ means that energy consumed for signaling and reception equals the energy consumed for transmitting data. Finally, the energy efficiency of PSM is larger than that of SF10 and SF12, this is because the payload bit rate of NBIoT is much larger than that of LoRaWAN. But, the energy efficiency of SF7 is higher than that of PSM though the bit rate of SF7 (about 5.47 kbps) is much smaller than that of NBIoT UEs. This is because LoRaWAN is a simple efficient protocol for networks and UEs can use almost all their energy on transmitting data.

We now consider an example Li-ion battery (typical supply voltage is 3.6 V) with capacity of 1000 mA-hour. The valid voltage range is 1.2 V, i.e. from 4.2 V to 3.0 V for Li-ion batteries. The transfer efficiency of modern power supply circuits is often more than 90% (common for switch-mode PSUs if the input power supply is stable and the difference in voltage between input and output is small). To be cautions, we set the PSU average transfer efficiency to 80% with a fixed output voltage. Each UE transmits 2 packets of 125 bytes per day. Based on Eq. (22), the battery lifetime is estimated in the Fig. 10.

In Fig. 10, the blue bars denote that the probability of active UEs p_a is 0.01 and yellow bars denote $p_a =$

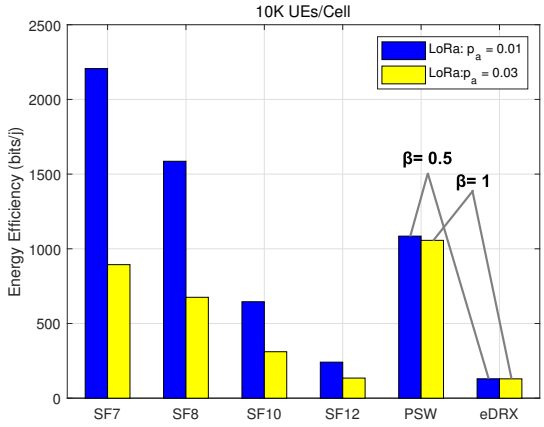

Figure 9: Energy efficiency for LoRaWAN UEs with different SF and for NBIoT UEs with different sleep modes.

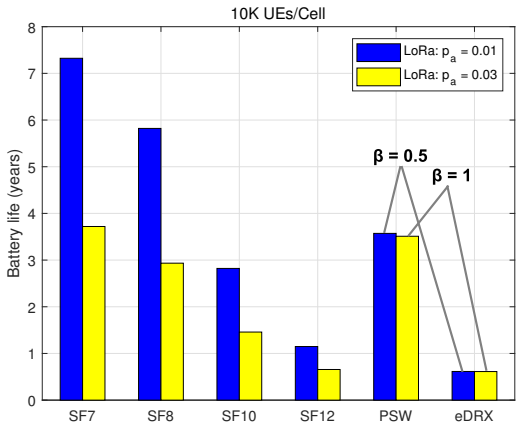

Figure 10: Battery lifetime for LoRaWAN UEs with different SF and for NBIoT UEs with different sleep modes.

0.03 for LoRaWAN and the blue bars denote $\beta = 0.5$ and the yellow bars denote $\beta = 1$ for NBIoT. We see that the most useful modes for long-life IoT applications in interference limited scenarios are NBIoT PSM mode and LoRa modes SF7 and SF8 (10k UEs/cell and average 100 active UEs/cell).

The coverage probability is another factor which influence the energy efficiency. For LoRaWAN networks, from the Eq. (7) and Fig. 6, the coverage probability can be increased by increasing the density of BSs when the density of UEs and the probability of active UEs is fixed. As shown in Fig. 11, the battery lifetime increases with the increasing of density of BSs in LoRaWAN networks, this is because increasing the density of BSs will increase the coverage probabilities, i.e. reduce the average number of retransmissions. The coverage probability of SF12 is highest in Fig. 6 but increases most slowly as function of BSs density as shown in Fig. 11. It also has the lowest energy efficiency as shown in Fig. 7 and Fig. 9. The battery lifetime of SF12 is the shortest and hardly influenced by the density of BSs. This is because SF12 spread spectrum communications improve the coverage probability at the expense of bit rate and energy but using longer codes.

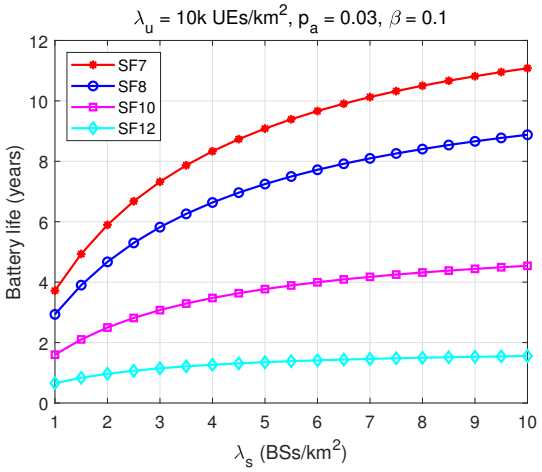

Figure 11: How battery lifetime varies with the density of BSs (range from 1 BS to 10 BS per km^2) in LoRaWAN networks. If the SF is larger, the battery lifetime is shorter and increases more slowly with the increasing of λ_s.

We did not compare the numerical results of energy efficiency and battery lifetime with Monte Carlo simulation because we can not simulate the full processes of LoRaWAN networks and NBIoT networks. Furthermore, there are no such large scale real networks to measure the data. As mentioned in section 4, the energy efficiencies in this paper are not the real networks' energy efficiency but an approximate estimation facilitating comparison (In fact, such energy predictions can not be obtained by mathematical model analysis or from measuring real networks since it depends on large numbers of parameters and changes with diverse networks at different times). Our purpose here is to provide some valuable guides to the design of real networks.

6 Conclusions

In this paper, we first proposed a framework and a conditional homogeneous PPP to calculate the coverage probabilities in UL of LoRaWAN networks and NBIoT networks. We give the energy efficiency models, then estimate the battery lifetime based on our mathematical results. The numerical results show that the battery lifetime can not reach 10 years even if less than 250 bytes are transmitted by each UE with the maximum transmit power per day both in LoRaWAN networks and NBIoT networks. In NBIoT networks, there is no intra-cell interference so the UEs can transmit data with the maximum bit rate to improve the energy efficiency. Using the PSM in NBIoT networks, a UE approaches

about half energy efficiency of a LoRaWAN UE with SF7 modulation. NBIoT networks use licensed bands, leading to extra cost compared to LoRaWAN networks. But due to this spectrum, NBIoT can provide better QoS, a high bit rate, low latency.

LoRaWAN networks can provide fast network deployment for low cost, so may be suitable for areas not in the coverage of macro NBIoT BSs, or for the scenarios with many interferers. SF12 modulation can be demodulated at -20dB SIR, which ensures LoRaWAN networks can work in poor link budget circumstance or with severe interference (as may be experienced in unlicensed shared spectrum). Furthermore, increasing the density of BSs in LoRaWAN networks, to reduce the UE energy consumption is a simple and economic method due to their lower cost. Finally, both LoRaWAN UEs and NBIoT UEs must transmit data at as high bit rate as possible to reduce the energy consumption.

The energy efficiency and battery lifetime models are affected by many factors. Our models are limited due to mainly considering the energy consumption of sending and receiving, the energy consumption of devices in sleep mode and in active model for data sensing and processing. Moreover, we only consider the devices sending data with fixed transmit power. In our future works, we will model and analysis the LPWAN where devices send data with power control according some factors, for example, the distance from devices to their BSs (or Gateways).

Appendix A. Proof of Theorem 1

Let $I_c = \sum_{x\in\Phi_{\mathrm{I}}} h_x R_x^{-\alpha}$, based on the definition, the coverage probability is expressed as

$$\begin{aligned} P_c(T) &= \mathbb{E}_r\left[(\mathrm{SIR} > T\,|r\,)\right] \\ &= \int_0^\infty \mathbb{P}\left[\frac{hr^{-\alpha}}{I_c} > T\,|r\right] f_R\left(r\right) dr \\ &= \int_0^\infty \mathbb{P}\left[h > Tr^\alpha I_c\,|r\,\right] f_R\left(r\right) dr. \end{aligned} \tag{25}$$

The $\mathbb{P}\left[h > Tr^\alpha I_c\,|r\,\right]$ in Eq. (25) can be expressed as

$$\begin{aligned} \mathbb{P}\left[h > Tr^\alpha I_c\,|r\,\right] &= \mathbb{E}_r\left[\mathbb{P}\left(h > Tr^\alpha I_c\,|r\,, I_c\right)\right] \\ &\underline{\underline{(a)}} \mathbb{E}_r\left[\exp\left(-Tr^\alpha I_c\,|r\,\right)\right] \\ &\underline{\underline{(b)}} \mathcal{L}_{I_c}\left(Tr^\alpha\right), \end{aligned} \tag{26}$$

where (a) follows from $h \sim \exp\left(1\right)$ and (b) follows from the definition of Laplace transform of PPP. Based on the distribution of interfering UEs in LoRaWAN networks (which is discussed in section 2.1), the Laplace transform $\mathcal{L}_{I_c}$ is express as

$$\begin{aligned} &\mathcal{L}_{I_c}\left(Tr^\alpha\right) \\ &= \mathbb{E}_{I_c}\left[e^{-Tr^\alpha I_c}\right] = \mathbb{E}_{\Phi_{\mathrm{I}},h_x}\left[-Tr^\alpha \sum_{x\in\Phi_{\mathrm{I}}} h_x R_x^{-\alpha}\right] \\ &= \mathbb{E}_{\Phi_{\mathrm{I}}}\left[\prod_{x\in\Phi_{\mathrm{I}}} \mathbb{E}_h\left[\exp\left(-Tr^\alpha h R_x^{-\alpha}\right)\right]\right] \\ &\overset{(c)}{=} \exp\left(-2\pi\frac{2p_a\lambda_u}{N_c N_f}\int_0^\infty \left(1-\mathbb{E}_h\left[\exp\left(-Tr^\alpha h v^{-\alpha}\right)\right]\right) v dv\right) \\ &= \exp\left(-\frac{2p_a\lambda_u}{N_c N_f}\pi r^2 \cdot \int_0^\infty \frac{T^{2/\alpha}}{1+x^{\alpha/2}} dx\right) \\ &= \exp\left(-\frac{2p_a\lambda_u}{N_c N_f}\pi r^2 \cdot T^{2/\alpha} \cdot \frac{2\pi\cdot\csc\left(2\pi/\alpha\right)}{\alpha}\right), \end{aligned} \tag{27}$$

where (c) follows from the Probability Generating Functional (PGFL).

All UEs choose their closest BSs with which to communicate, and based on Andrews, J.G. et al. (2011), the PDF of the distance from UE to its closest BS is

$$f_R\left(r\right) = 2\lambda_s \pi e^{-\lambda_s \pi r^2}. \tag{28}$$

Combining Eq. (27) and (28) into (25) yields (7).

The coverage probability of NBIoT is similar to the above proof, we can directly find the coverage probability as

$$P_d\left(T\right) = \int_0^\infty \mathcal{L}_{I_d}\left(Tr^\alpha\right) f_R(r) dr. \tag{29}$$

Based on the distribution of interfering UEs in NBIoT networks (which is discussed in section 2.2), the $\mathcal{L}_{I_d}$ is derived as follows:

$$\begin{aligned} &L_{I_d}\left(Tr^\alpha\right) \\ &= \exp\left(-2\lambda_s\pi\int_{\frac{1}{2\sqrt{\lambda_s}}}^\infty \left(1-\frac{1}{1+Tr^\alpha v^{-\alpha}}\right) v dv\right) \\ &= \exp\left(-\lambda_s\pi r^2 T^{2/\alpha}\int_b^\infty \frac{1}{1+\left(\frac{v^2}{r^2}T^{-2/\alpha}\right)^{\alpha/2}} d(\frac{v^2}{r^2}T^{-2/\alpha})\right), \end{aligned} \tag{30}$$

where $b = \frac{\pi}{4\lambda_s\pi r^2 T^{2/\alpha}}$, combining Eq. (30) and (28) into (29) and let $u = T^{-2/\alpha}\cdot v^2/r^2$ and $x = \lambda_s\pi r^2$ yields (8) and (9).

References

Gharbieh, M., Elsawy, H., Bader, A. and Alouini, M.S. (2016) 'Tractable stochastic geometry model for IoT access in LTE networks', *2016 IEEE Global Communications Conference (GLOBECOM)*, pp.1–7.

Gantz J. and Reinsel D. (2012) 'The digital universe in 2020: Big data, bigger digital shadows, and biggest growth in the far east', *IDC iView: IDC Analyze the Future*, pp.1–16.

Taylor, S. (2013) 'The next Generation of the internet revolutionizing the way we work, live, play, and learn', *CISCO Point of View*, pp.1–7.

Al-Fuqaha, A., Guizani, M. Mohammadi, M., Aledhari, M. and Ayyash, M. (2015) 'Internet of things: A survey on enabling technologies, protocols and applications', *IEEE Communications Surveys and Tutorials*, Vol. 17, No. 4, pp.2347–2376.

Sinha, S.H., Wei, Y.Q. and Hwang, S.H. (2017) 'Internet of things: A survey on LPWA technology: LoRa and NB-IoT', *ICT Express*, Vol. 3, No. 1, pp.14–21.

Mekki, K., Bajic, E., Chaxel, F. and Meyer, F. (2018) 'A comparative study of LPWAN technologies for large-scale IoT deployment', *ICT Express*.

Andrews, J. G., Abhishek K.G. and Harpreet S.D. (2016) 'A primer on cellular network analysis using stochastic geometry', *arXiv preprint arXiv:1604.03183*.

Kamalinejad, P., Mahapatra, C., Sheng, Z.G., Mirabbasi, S.L., Victor C. M. and Guan, Y.L. (2015) 'Wireless energy harvesting for the Internet of Things', *IEEE Communications Magazine*, Vol. 53, No. 6, pp.102–108.

Kroll, H., Korb, M., Weber, B., Willi, S. and Huang, Q.T. (2017) 'Maximum-likelihood detection for energy-efficient timing acquisition in NB-IoT', *Wireless Communications and Networking Conference Workshops*, pp.1–5.

Hu, H.N., Weng, J.L. and Zhang, J. (2016) 'Coverage performance analysis of FeICIC low-power subframes', *IEEE Transactions on Wireless Communications*, Vol. 15, No. 8, pp.5603–5614.

Andrews, J.G., Bai, T.Y., Kulkarni, M.N., Alkhateeb, A., Gupta, A.K. and Heath, R.W. (2017) 'Modeling and analyzing millimeter wave cellular systems', *IEEE Transactions on Communications*, Vol. 65, No. 1, pp.403–430.

Nigam, G., Minero, P. and Haenggi, M. (2014) 'Coordinated multipoint joint transmission in heterogeneous hetworks', *IEEE Transactions on Communications*, Vol. 62, No. 11, pp.4134–4146.

Salehi, M., Mohammadi, A. and Haenggi, M. (2017) 'Analysis of D2D underlaid cellular networks: SIR meta distribution and mean local delay', *IEEE Transactions on Communications*, Vol. 65, No. 7, pp.2904–2916.

George, G., Mungara, R.K., Lozano, A. and Haenggi, M. (2017) 'Ergodic spectral efficiency in MIMO cellular networks', *IEEE Transactions on Wireless Communications*, Vol. 16, No. 5, pp.2835–2849.

Li, Z.C., Zozor, S., Drossier, J.M., Varsier, N. and Lampin, Q. (2017) '2D time-frequency interference modelling using stochastic geometry for performance evaluation in low-power wide-area networks', *IEEE International Conference on Communications*, pp.1–7.

Gharbieh, M., Elsawy, H., Bader, A., and Alouini, M.S. (2017) 'Spatiotemporal stochastic modeling of IoT enabled cellular networks: scalability and stability analysis', *IEEE Transactions on Communications*, Vol. 65, No. 8, pp.3585–3600.

Bai, T., and Heath, R.W. (2016) 'Analyzing uplink SINR and rate in massive MIMO systems using stochastic geometry', *IEEE Transactions on Communications*, Vol. 64, No. 11, pp.4592–4606.

ElSawy, H. and Hossain, E. (2014) 'On stochastic geometry modeling of cellular uplink transmission with truncated channel inversion power control', *IEEE Transactions on Wireless Communications*, Vol. 13, No. 8, pp.4454–4469.

Lee H. Y., Sang, Y.J. and Kim, K.S. (2014) 'On the uplink SIR distributions in heterogeneous cellular networks', *IEEE Transactions on Wireless Communications*, Vol. 18, No. 12, pp.2145–2148.

Singh, S., Zhang, X.C. and Andrews, J.G. (2015) 'Joint rate and SINR coverage analysis for decoupled uplink-downlink biased cell associations in HetNets', *IEEE Transactions on Wireless Communications*, Vol. 14, No. 10, pp.5360–5373.

Wang, Y.J., Haenggi, M. and Tan, Z.H. (2017) 'The meta distribution of the SIR for cellular networks with power control', *IEEE Transactions on Communications*, pp.1–12.

Haenggi, M. (2017) 'User point processes in cellular networks', *IEEE Wireless Communications Letters*, Vol. 6, No. 2, pp.258–261.

Andrews, J.G., Baccelli, F. and Ganti, R.K. (2011) 'A tractable approach to coverage and rate in cellular networks', *IEEE Transactions on Communications*, Vol. 59, No. 11, pp.3122–3134.

LoRa Alliance (2016) 'LoRaWAN 1.0.2: Regional parameters', *Standard*.

Semtech Co. (2015) 'SX1276/77/78/79 data sheet'.

R. S. Sinha, Y. Wei. and S. H. Hwang (2017) 'Narrowband internet of things', *Whitepaper, 3GPP*, August 2016.

3GPP (2016) 'Physical layer procedures', TS 36.213, Vol. 13.2.0, June, 2016.

3GPP (2017) 'General packet radio service GPRS enhancements for evolved universal terrestrial radio access network E-UTRAN access', TS 23.401, Vol. 15.1.0, September, 2017.

3GPP (2017) 'Architecture enhancements to facilitate communications with packet data networks and applications', TS 23.682, Vol. 15.2.0, September, 2017.

3GPP (2017) 'Mobile radio interface layer 3 specification; Core network protocols; Stage 3', TS 24.008, Vol. 15.0.0, September, 2017.

3GPP (2017) 'Non-access-stratum NAS protocol for evolved packet system EPS; Stage 3', TS 24.301, Vol. 15.0.1, September, 2017.

Ublox Ltd. (2017) 'SARA-N2 power-optimized NBIoT LTE Cat NB1 modules Data Sheet', October, 2017.

Martin Haenggi (2012) 'Stochastic geometry for wireless networks', *Cambridge University Press*.

François B. and Bartllomiej B. (2009) 'Stochastic geometry and wireless networks: Volume I Theory', *Now Publishers*.

Burdett A. (2015) 'Ultra-low-power wireless systems: Energy-efficient radios for the Internet of Things', *IEEE Solid-State Circuits Magazine*, Vol. 7, No. 2, pp.18–28.

Lauridsen, M., Kovacs, I.Z., Mogensen, P., Sorensen, M. and Holst, S. (2015) 'Ultra-low-power wireless systems: Energy-efficient radios for the Internet of Things', *2016 IEEE 84th Vehicular Technology Conference (VTC-Fall)*, pp.1–5.

Baccelli, F., Blaszczyszyn, B., and Muhlethaler, P. (2009) 'Stochastic analysis of spatial and opportunistic Aloha', *IEEE Journal on Selected Areas in Communications*, Vol. 27, No. 7, pp.1105–1119.

Elsawy, H. and Hossain, E. (2014) 'On stochastic geometry modeling of cellular uplink transmission with truncated channel inversion power control', *IEEE Transactions on Wireless Communications*, Vol. 13, No. 8, pp.4454–4469.

Novlan, T.D., Dhillon, H.S. and Andrews, J.G. (2013) 'Analytical modeling of uplink cellular networks', *IEEE Transactions on Wireless Communications*, Vol. 12, No. 6, pp.2669–2679.

Haenggi, M. (2016) 'The meta distribution of the SIR in Poisson bipolar and cellular networks', *IEEE Transactions on Wireless Communications*, Vol. 15, No. 4, pp.2577–2589.